ELSEVIER

Journal of Membrane Science 182 (2001) 77–90

journal of MEMBRANE SCIENCE

www.elsevier.nl/locate/memsci

Reverse osmosis filtration for space mission wastewater: membrane properties and operating conditions

Sangho Lee, Richard M. Lueptow*

Department of Mechanical Engineering, Northwestern University, Evanston, IL, 60208, USA

Received 16 May 2000; received in revised form 20 July 2000; accepted 8 August 2000

Abstract

Reverse osmosis (RO) is a compact process that has potential for the removal of ionic and organic pollutants for recycling space mission wastewater. Seven candidate RO membranes were compared using a batch stirred cell to determine the membrane flux and the solute rejection for synthetic space mission wastewaters. Even though the urea molecule is larger than ions such as Na^+, Cl^-, and NH_4^+, the rejection of urea is lower. This indicates that the chemical interaction between solutes and the membrane is more important than the size exclusion effect. Low pressure reverse osmosis (LPRO) membranes appear to be most desirable because of their high permeate flux and rejection. Solute rejection is dependent on the shear rate, indicating the importance of concentration polarization. A simple transport model based on the solution–diffusion model incorporating concentration polarization is used to interpret the experimental results and predict rejection over a range of operating conditions. © 2001 Elsevier Science B.V. All rights reserved.

Keywords: Water treatment; Reverse osmosis; Concentration polarization; Rejection

1. Introduction

For long-duration space missions, a Water Recovery and Management System (WRMS) will be necessary to reduce the dependency on resupply of water and provide an ongoing safe and healthy water supply [1]. Early space missions were of such short duration that stored water was used for the mission. But this approach cannot be applied to missions of long duration or having large crews [2]. Thus, recycling of wastewater to produce potable water as well as water for washing will be crucial in long term space missions.

However, it is quite difficult to produce high quality water from the space mission wastewater. Fig. 1 shows the contribution to the wastewater streams in manned spacecraft [3]. The inputs to the wastewater stream include waste hygiene water, condensate water, and urine. The pollutants in the wastewater can pose a threat to human health. Organic and inorganic contaminants such as urea, ammonia, halogenated carbons, and heavy metals are of concern because of their harmful effects on humans. Microorganisms that may be pathogenic or clog water lines are also of concern. Furthermore, design requirements of the WRMS are very stringent [4]. The WRMS should be inherently reliable, capable, and efficient. The use of expendables should be minimal. Minimizing the total weight, volume, power consumption, and cost of the system while ensuring safe operation is necessary. Mass loop closure, in which nearly all water is reclaimed, is essential for long-term missions. Although various technologies have been attempted for the

* Corresponding author.
E-mail address: r-lueptow@northwestern.edu (R.M. Lueptow).

0376-7388/01/$ – see front matter © 2001 Elsevier Science B.V. All rights reserved.
PII: S0376-7388(00)00553-6

Nomenclature

A_m	Membrane area (m^2)
C_b	Solute concentration in the bulk phase (kg/m^3)
C_f	Feed concentration (kg/m^3)
C_m	Solute concentration at membrane surface (kg/m^3)
C_p	Solute concentration at permeate side (kg/m^3)
D_{sw}	Diffusion coefficient of solute (m^2/s).
f_c	Concentration factor
J_s	Solute flux (m/s)
J_v	Solvent flux (m/s)
k	Mass transfer coefficient on high pressure side of membrane
L_s	Solute transport parameter (m/s)
L_v	Solvent transport parameter (m^2-s/kg)
ΔP	Transmembrane pressure (Pa)
ΔP_{eff}	Effective transmembrane pressure (Pa)
r	Radius of stirred cell (m)
R	Solute rejection
t	Time (s)
V_c	Volume of concentrate (m^3)
V_f	Volume of initial feed (m^3)
V_p	Volume of total permeate (m^3)

Greek letters

$\Pi(C_m)$	Osmotic pressures at the solute concentration of C_m (Pa)
$\Pi(C_p)$	Osmotic pressures at the solute concentration of C_p (Pa)
ρ	Solution density (kg/m^3)
μ	Solvent viscosity (kg/m-s)
ω	Stirring velocity (rad/s)

wastewater recycling in space [5–8], few technologies meet the stringent requirements for space application.

Recently, reverse osmosis (RO) membrane technology has drawn attention because of its advantages over other processes. RO membrane filtration is a regenerable technology that requires replacement far less often than conventional filtration (usually 1–2 per year in commercial membrane plants). RO filtration also removes ions, proteins, and organic chemicals which are generally very difficult to remove using conventional treatment. Moreover, RO is an absolute filtration method, so its treatment efficiency and performance are stable and predictable.

However, there are several problems to be resolved in the application of RO membranes to a WRMS. The physico-chemical basis for RO is much more complex than for other filtration techniques. Rejection by RO depends on the physical chemistry of the solvent, solute, and membrane as well as physical size difference between solute and membrane pore. For ionic solutes, the degree of separation depends not only on the hydrated size of the ion, but also on the ionic charge. For organic solutes, the chemical affinity of the solute for the membrane material is as important as the molecular weight of the solute. Therefore, a fundamental understanding of the chemical and physical mechanisms governing the rejection of pollutants in space mission wastewater by RO is of paramount practical importance.

Determination of the optimum operating condition is another important issue, especially for the application of wastewater recycle and reuse [9–11]. Since space and energy are quite restricted in space missions, the operating conditions such as transmembrane pressure and shear rate should be carefully selected.

The objective of this research is to establish the characteristics of RO membranes for the rejection of organic and inorganic compounds in space mission wastewater. The results are analyzed in terms of the combined film theory/solution–diffusion theory.

2. Experimental methods

Seven RO membranes were compared in terms of their effectiveness in treating synthetic wastewater using a batch stirred cell. Two wastewater solutions were used as model synthetic wastewater, as shown in Table 1. The chemical composition of the synthetic wastewater was based on analysis of actual wastewater in spacecraft [6,12]. Wastewater A represents the wastewater before ammonification. The wastewater includes a high concentration of urea as well as NaCl and NASA body soap (sodium–coconut acid–*N*-methyl taurate). Wastewater B represents the wastewater after ammonification. Urea and crea-

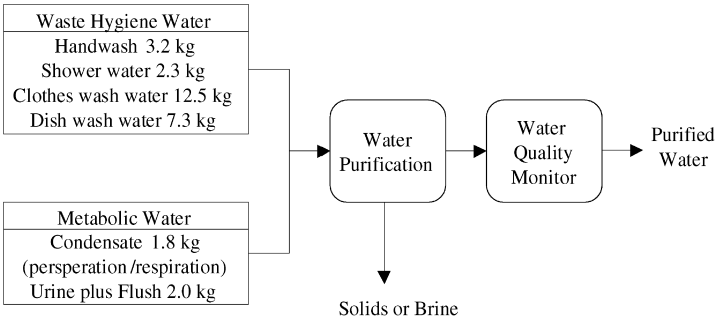

Fig. 1. Daily wastewater inputs to the Water Recovery and Management System for one person [3].

tine were replaced by ammonium carbonate so that the total concentration of nitrogen was the same as Wastewater A. All other compounds (NASA body soap and NaCl) were maintained at the same concentration in both wastewater solutions. All synthetic wastewater was used within 8 h to prevent any change in composition.

Membrane characteristics for the seven RO membranes that were tested are listed in Table 2. All membranes were of the thin film composite (TFC) type. The polymer make-up of the membranes according to the manufacturers is polyamide except NTR729HF, which is made of polyvinyl alcohol.

The experiments were performed in batch mode using a stirred cell as shown in Fig. 2. A stirred cell module was used because the shear stress could be easily controlled. The stirred cell was made of aluminum and coated with Teflon to improve chemical stability. The diameter of the stirred cell was 54 mm and the working volume was 50 ml. A magnetic stirrer (Stirrer assembly 8200, Millipore, USA) was positioned just above the membrane. The length of the stirring bar was 52 mm. The working pressure was controlled by a high pressure nitrogen cylinder and by a gas pressure regulator. The stirring speed was controlled by a magnetic stirrer plate. The temperature of the feed solution was adjusted to 20–25°C and the effect of temperature on viscosity and density was corrected. Since the experiment was performed in a short time (normally less than 30 min), the variations of the temperature during an experiment were smaller than ±1°C.

A fresh membrane was first rinsed by letting it float skin-side down in distilled water for 30 min. Then it was placed in the stirred cell. The stability of the mem-

Table 1
Composition of synthetic wastewater

Components	Dosage (mg/l)	Theoretical TOC (mg/l)	Theoretical total nitrogen (mg/l)
Wastewater A			
Urea	2000	400	932
Creatine	200	85	74
NASA body soap	2000[a]	100	38
NaCl	1000	0	0
Total	5200	585	1044
Wastewater B			
$(NH_4)_2CO_3$	3429	0	1000
NASA body soap	2000[a]	100	38
NaCl	1000	0	0
Total	6429	100	1038

[a] 2000 mg/l dosage of the NASA soap corresponds to 162.6 mg/l as linear alkylbenzene sulfonate (LAS) according to HACH detergent analysis method (crystal violet method).

Table 2
List of RO membranes and their characteristics obtained from manufacturers

Type of RO	Membrane		pH range	Normal/maximum operating pressure (kPa)
	Product name	Manufacture		
Brackish water	BW30	Dow	2–11	1550/6000
Low pressure	ESPA	Hydranautics	3–10	1050/4160
Nanofiltration	NTR729HF	Hydranautics	3–10	1550/4000
Brackish water	ATFRO	AMT	3–10	1550/5480
Brackish water	ATFRO-HR	AMT	3–10	1550/5480
Brackish water	HR95	DDS	3–10	–
Low pressure	ACM4	TriSep corp.	4–11	680/4100

brane permeability during the experiment was checked by comparing pure water flux before and after the experiment. Only those membranes for which permeability changes were less than 10% were included in the data presented here.

The permeate flux was measured using a graduated cylinder and is expressed in terms of concentration factor (f_c). The concentration factor, defined as a ratio of the feed volume to concentrate volume, indicates the extent of concentration:

$$f_c = \frac{V_f}{V_c} = 1 + \frac{V_p}{V_c} \quad (1)$$

where V_f, V_c, and V_p are defined as the volume of feed, concentrate, and permeate, respectively. The solute concentrations of the permeate were measured at different concentration factors.

After filtration tests, all samples were acidified below the pH of 2.0 by adding 10% sulfuric acid to prevent the loss of nitrogen compounds for analysis.

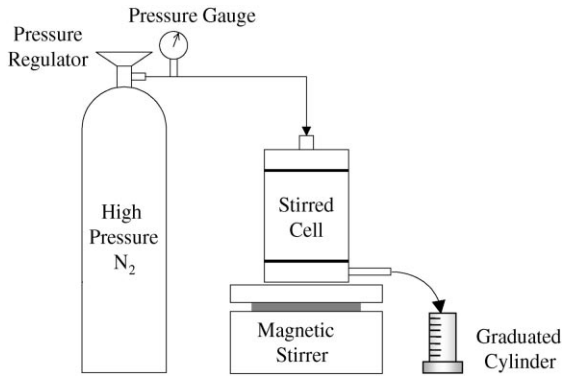

Fig. 2. Schematic diagram of stirred cell RO device.

Analysis of ammonium ions was conducted using the procedures described in Standard Methods [13]. A total organic carbon (TOC) analyzer (DC-180, Dohrmann, USA) was used for measurement of organic contents in the synthetic wastewater and permeates. The spectrophotometric method of Hach [14] was adapted to measure the total nitrogen concentration, detergent concentration, and chloride ion concentration in feed and permeate. In addition, the concentrations of other ionic compounds were determined by conductivity measurements and were automatically corrected for temperature influence. These concentrations were used to calculate the rejection R, according to

$$R = 1 - \frac{C_p}{C_f} \quad (2)$$

where C_p is the concentration in the permeate and C_f the concentration in the feed.

3. Results and discussion

3.1. RO membrane characterization

In order to compare the basic properties of the RO membranes, salt rejection measurements based on electrical conductivity were carried out for Na_2SO_4, NaCl and $CaCl_2$ under the following operating conditions: the transmembrane pressure, 800 kPa; stirring speed, 400 rpm; recovery (the ratio of total permeate volume to initial feed volume), 60%. The results are shown in Fig. 3. These salt rejection measurements permit the classification of most of the membranes into two categories, as suggested by Peeters et al. [15] for nanofiltration (NF) membranes:

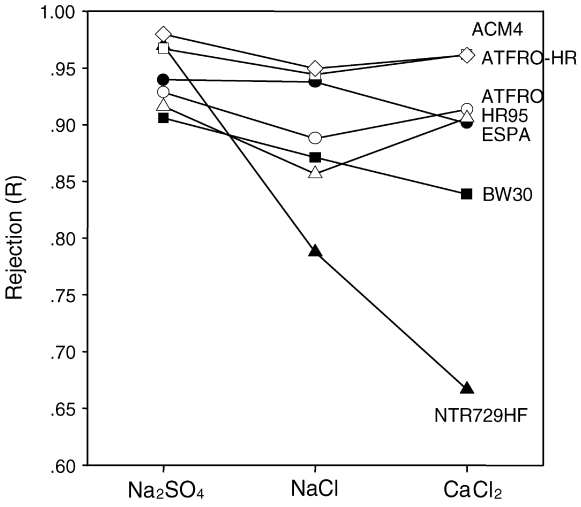

Fig. 3. Rejection of different salts for various RO membranes. Operating conditions: ΔP, 800 kPa; stirring speed, 400 rpm; salt concentration: 0.02 M; 60% recovery. ((●): ESPA; (■): BW30; (▲): NTR729HF; (○): ATFRO; (□): ATFRO-HR; (△): HR95; (◇): ACM4).

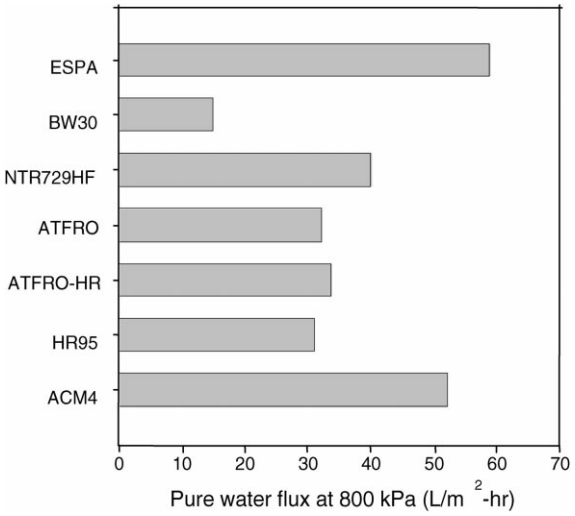

Fig. 4. Pure water flux for various RO membranes. Operating conditions: Δ*P*, 800 kPa.

- Category I: Membranes for which electrostatic interaction such as Donnan exclusion plays an important role.
- Category II: Membranes for which the rejection is determined by differences in diffusion coefficients between the salts.

Since the difference between two categories results from the Donnan effect, this classification represents a charge property of RO membranes: Category I membranes have more charge density than Category II membranes. Membranes falling into Category I have the salt rejection order typical for a negatively charged membrane: $R(Na_2SO_4) > R(NaCl) > R(CaCl_2)$. The membranes of this category are ESPA, BW30 and NTR729HF, which are designated by filled symbols in Fig. 3. The high rejection for the Na_2SO_4 and the low rejection for $CaCl_2$ are in accordance to the Donnan exclusion model. This type of rejection sequence has been reported by several other authors and is attributed to the strong negative charge of the membranes [16].

The rejection sequence for Category II membranes is caused by differences in diffusion coefficients between the salts. The diffusion coefficients decrease from NaCl ($1.61 \times 10^{-9}\,m^2/s$) to $CaCl_2$ ($1.45 \times 10^{-9}\,m^2/s$) to Na_2SO_4 ($1.23 \times 10^{-9}\,m^2/s$) [15]. This order of diffusion coefficients is inversely reflected in the salt rejection order: $R(Na_2SO_4) > R(CaCl_2) > R(NaCl)$. This salt rejection order is characteristic of ATFRO, ATFRO-HR, HR95, and ACM4 membranes, designated by open symbols in Fig. 3.

The pure water flux for the membranes is shown in Fig. 4. The measured pure water flux is 1.2–3-times higher than the flux from membrane manufactures, because the flux data from the manufacturers are measured in spiral wound modules under different conditions from those we used. The water fluxes of the ESPA and ACM4 membranes are high compared to other membranes. These membranes also have relatively high salt rejection, as indicated in Fig. 3. The NTR729HF membrane also has high water permeability, but its salt rejection is low, especially in case of a divalent cation ($CaCl_2$).

3.2. Comparison of RO membranes using synthetic Wastewater A (containing urea)

Fig. 5 shows the decline in the flux with increasing concentration factor for the filtration of synthetic Wastewater A, which contains urea. The permeate flux for the wastewater was significantly reduced compared to the pure water flux. The flux at a concentration factor of 2.5 was in the range of 13–56%, that for pure

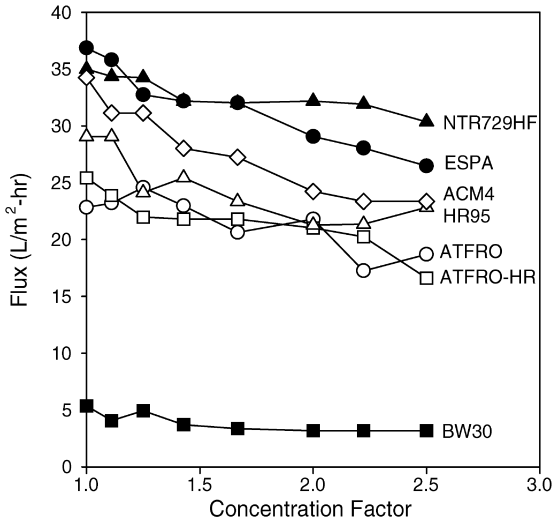

Fig. 5. Flux decline for reverse osmosis of synthetic Wastewater A (containing urea and creatine) for different membranes. Operating conditions: ΔP, 800 kPa; stirring speed, 400 rpm ((●): ESPA; (■): BW30; (▲): NTR729HF; (○): ATFRO; (□): ATFRO-HR; (△): HR95; (◇): ACM4).

water. Most likely, the osmotic pressure plays a major role in the lower flux by reducing the effective transmembrane pressure.

The compositions of the permeate for the RO membranes are summarized in Table 3. The rejections are indicated in parentheses. The rejection of detergent was over 0.97 for all membranes. This is because the detergent molecules in NASA body soap (mainly sodium–coconut acid–*N*-methyl taurate) are large enough to be rejected via size exclusion for most RO membranes. According to Archer et al. [17], over 0.95 detergent rejection can be obtained even using NF membranes. The ion rejection, measured as conductivity and chloride rejection, was also high. The exception is the NTR729HF membrane, which is a NF membrane and is thus expected to have a larger salt permeability.

Rejections of total organic carbon (TOC) and total nitrogen (TN) were not as high as the rejection of detergent and ions. TOC rejections ranged from 0.44 (NTR729HF) to 0.80 (ATFRO-HR) and TN rejections were from 0.25 (NTR729HF) to 0.74 (ACM4). This indicates that the organic nitrogen compounds, (mainly urea), are rather difficult to reject using RO membranes. The lower rejection of urea is probably related to the chemical affinity of the urea molecules to the membrane material.

There is little difference between Category I (ESPA, BW30 and NTR729HF) and Category II membranes (ATFRO, ATFRO-HR, HR95 and ACM4). This is probably a consequence of the wastewater containing mostly monovalent ions and non-charged organics. Because the Donnan effect becomes important with divalent ions, the membrane charge properties are of little importance for treating the wastewater.

Table 3
Comparison of permeate qualities in various RO treatments for synthetic Wastewater A[a]

	TOC (mg/l)	TN (mg/l)	Conductivity (mS/cm)	Chloride (mg/l)	Detergent (mg/l)	Average flux (l/m^2/h)
Feed	570	980	2.1	553	162.6	
BW30	183	540	0.24	56.7	2.88	3.9
	(0.68)	(0.45)	(0.88)	(0.89)	(0.98)	
ATFRO	193	585	0.185	29.8	1.62	22.1
	(0.66)	(0.40)	(0.91)	(0.95)	(0.99)	
ATFRO-HR	113	285	0.063	7.8	0.99	22.0
	(0.80)	(0.71)	(0.97)	(0.99)	(0.99)	
ESPA	121	315	0.058	12.65	1.44	31.8
	(0.79)	(0.68)	(0.97)	(0.98)	(0.99)	
HR95	238	555	0.111	18.6	1.53	24.8
	(0.58)	(0.43)	(0.94)	(0.97)	(0.99)	
NTR729HF	318	735	0.434	130.6	5.46	33.0
	(0.44)	(0.25)	(0.79)	(0.76)	(0.97)	
ACM4	117	254	0.109	35	1.53	28.4
	(0.79)	(0.74)	(0.95)	(0.94)	(0.99)	

[a] Concentration factor: 2.5; ( ): rejection.

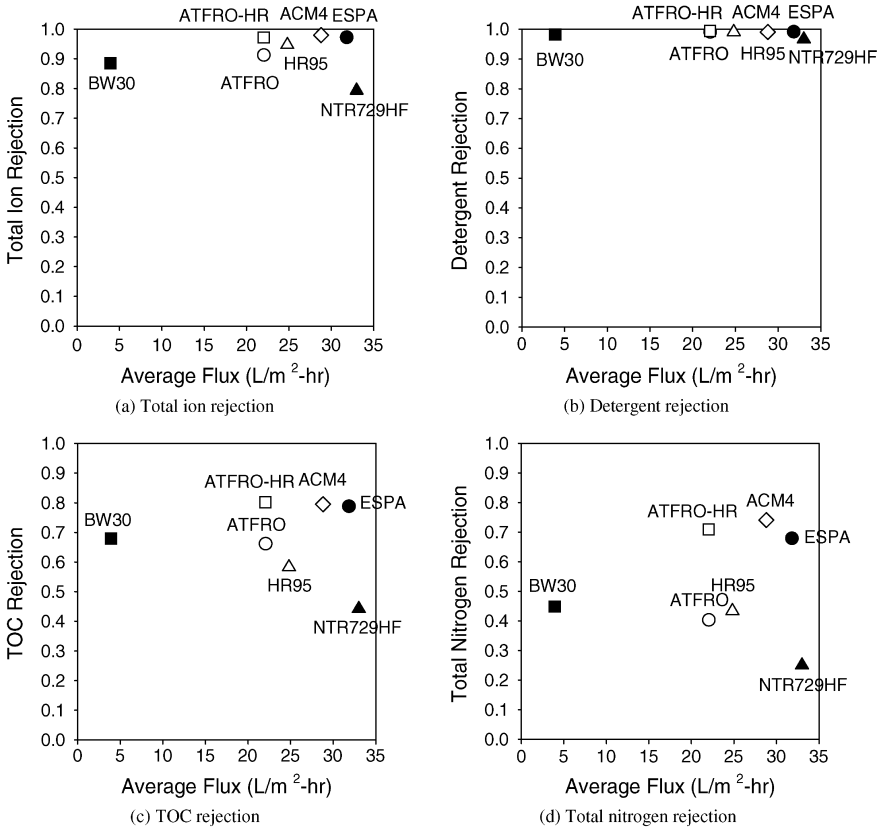

Fig. 6. Comparison of average flux and solute rejection by RO membranes with synthetic Wastewater A (containing urea and creatine). (a) Total ion rejection; (b) detergent rejection; (c) TOC rejection; (d) TN rejection. Operating conditions: ΔP, 800 kPa; stirring speed, 400 rpm; concentration factor, 2.5 ((●): ESPA; (■): BW30; (▲): NTR729HF; (○): ATFRO; (□): ATFRO-HR; (△): HR95; (◇): ACM4).

In spacecraft applications, it is essential to produce high quality water with high permeation rate because capacity and energy are limited. To determine suitable membranes, the rejections of ions, detergent, TOC, and TN are plotted as a function of average flux during RO filtration in Fig. 6. The NTR729HF membrane has the highest permeate flux but it has the lowest rejection of solutes. The BW30 membrane has the lowest flux, but this does not guarantee the highest rejection of solute. Only ESPA and ACM4 membranes have the high permeate flux with high rejection for all of the components of the synthetic wastewater. According to the manufacturers, these are low pressure reverse osmosis (LPRO) membranes. LPRO membranes differ from NF membranes in that NF membranes have high water flux but low rejection of monovalent ions while LPRO membranes have both high flux and high rejection. This is because the effective membrane area of LPRO membranes is several times larger than that of normal RO membranes due to a wavy surface at the microscopic scale [18]. The ESPA membrane appears better than the ACM4 membrane in that its flux is higher for all concentration factors, as shown in Fig. 5.

3.3. Comparison of RO membranes using synthetic Wastewater B (containing ammonium)

Ammonification is a crucial factor to be considered in a spacecraft water recovery application. During storage, urea and other organic nitrogen compounds are converted to ammonium ions in the presence of urease from microorganisms in the wastewater. Ammonification of urea can be described as

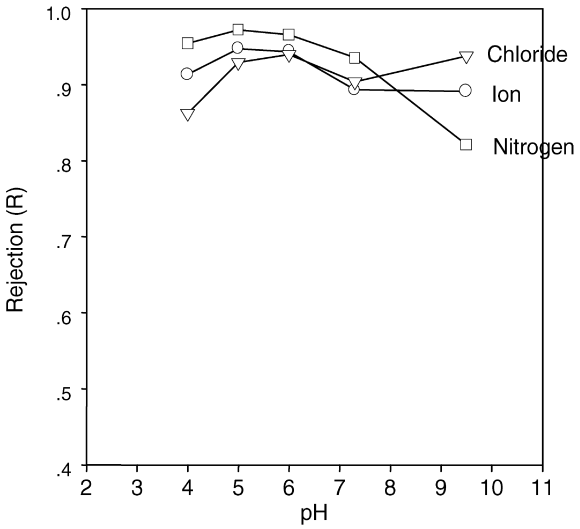

Fig. 7. Variation of solute rejection with respect to feed pH in case of the Wastewater B (containing NH_4^+) for the ESPA membrane ((○): total ion rejection; (▽): chloride rejection; (□): nitrogen rejection). Operating conditions: ΔP, 800 kPa; stirring speed, 400 rpm; concentration factor, 2.5.

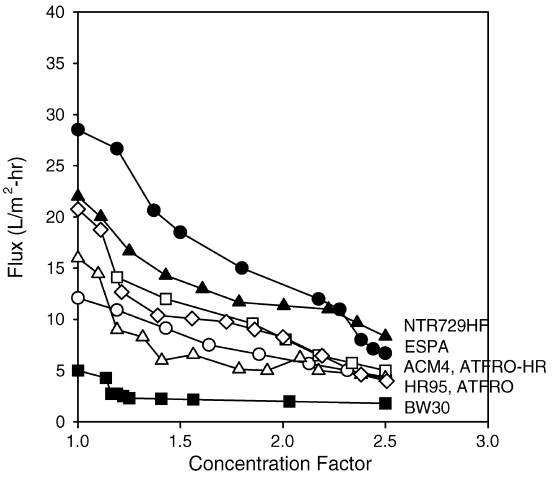

Fig. 8. Flux decline for reverse osmosis of synthetic Wastewater B (containing NH_4^+). Operating conditions: DP, 800 kPa; stirring speed, 400 rpm; concentration factor, 2.5 ((●): ESPA; (■): BW30; (▲): NTR729HF; (○): ATFRO; (□): ATFRO-HR; (△): HR95; (◇): ACM4).

follows [19]:

$$CO(NH_2)_2 + 3H_2O \overset{\text{Urease}}{\rightarrow} 2NH_4^+ + HCO_3^- + OH^- \quad (11)$$

Unlike other biological nitrogen conversions such as nitrification and denitrification, the decomposition of urea to ammonium is a relatively fast process [12,19]. Consequently, the rejection of ammonium ions by RO membranes must also be examined. In order to simulate the wastewater after ammonification, Wastewater B, which contains ammonium ions instead of urea and creatine, was tested under experimental conditions identical to those used for Wastewater A.

The synthetic wastewater containing $(NH_4)_2CO_3$ has a pH of 9.5 because of the bicarbonate ion. Thus, it is important to consider the effect of solution pH on solute rejection. To adjust the pH, 2N sulfuric acid was added to the wastewater. As shown in Fig. 7, the rejection of solutes by the ESPA membrane is dependent on the wastewater pH. As the pH of the feed solution decreases from 9.5 to 5, the nitrogen rejection and total ion rejection increase. A further decrease in the pH, however, results in decreased rejection. Similar results were obtained for the other membranes.

This result can be explained by considering the equilibrium characteristics of ammonia (NH_3) and ammonium ions (NH_4^+). At high pH, the dominant form of nitrogen compounds is ammonia, which is a neutral molecule and difficult to reject by RO. But as the solution pH decreases, the dominant form is the ammonium ion, because the ammonium ion is weak acid ($pK_a = 9.3$). Since ions can be rejected more easily by RO, the rejection increases as the pH is decreased. Since the pH adjustment prior to RO filtration results in better rejection, all subsequent experiments with the wastewater containing $(NH_4)_2CO_3$ were conducted after the pH was adjusted to 6.0.

Fig. 8 shows the flux as a function of concentration factor for RO filtration of Wastewater B. Comparing to Fig. 5, the initial flux is lower and the flux decline is more severe than for Wastewater A. This can be attributed to a higher osmotic pressure for ammonium ions than for urea, which reduces the effective transmembrane pressure. The osmotic pressure of the synthetic Wastewater A is 160 kPa while that of the synthetic Wastewater B 340 kPa. Not only does this increase the rate of decline of flux with concentration factor, it reduces the overall flux for Wastewater B.

The rejection of ions, detergent, organic carbon, and nitrogen is illustrated as a function of the permeate

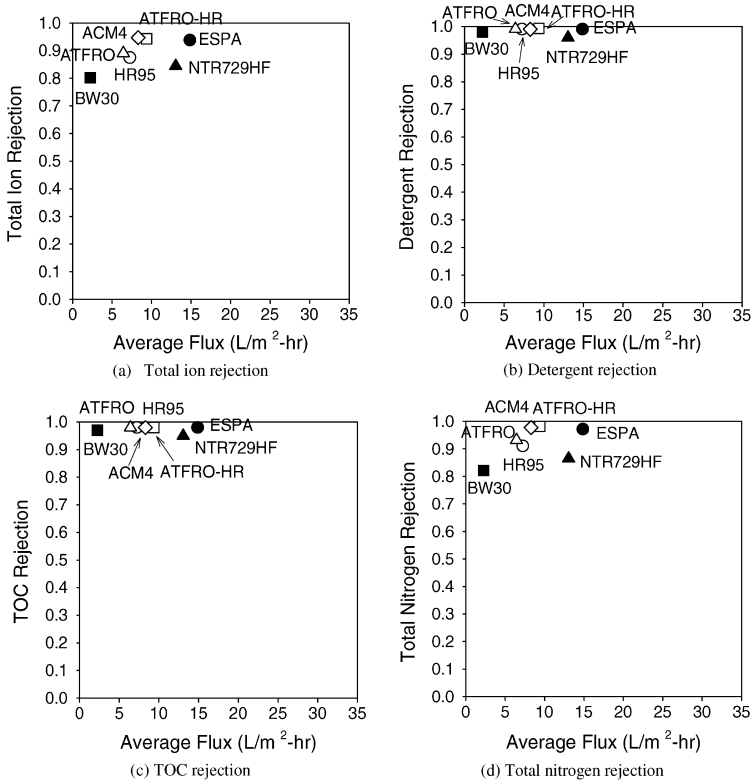

Fig. 9. Comparison of average flux and solute rejection by RO membranes with synthetic Wastewater B (containing NH_4^+). (a) Total ion rejection; (b) detergent rejection; (c) TOC rejection; (d) TN rejection. Operating conditions: ΔP, 800 kPa; stirring speed, 400 rpm, concentration factor, 2.5; pH, 6.0 ((●): ESPA; (■): BW30; (▲): NTR729HF; (○): ATFRO; (□): ATFRO-HR; (△): HR95; (◇): ACM4).

flux in Fig. 9 for synthetic Wastewater B. The rejection of nitrogen is significantly increased compared with the synthetic wastewater containing urea. This reflects the better rejection of ammonium ions than urea even though ammonium ions are smaller, since ionic compounds have less affinity to the membrane material than organic molecules. Like Wastewater A, ions and detergent have high rejection. The rejection of total organic carbon is also high because the total organic carbon in Wastewater B is in the detergent which is easily rejected. Like Wastewater A, there was also no significant difference between Category I and II membranes in treating Wastewater B, because the wastewaters contain mostly monovalent ions and organics which are less influenced by the Donnan effect. Again, the charge property of the membrane is not a significant factor to be considered in treating these wastewaters

As shown in Figs. 5 and 8, the flux for synthetic Wastewater B (containing ammonium) is much lower than that for synthetic Wastewater A (containing urea). However, the rejection is higher for ammonium than urea, as demonstrated in Fig. 6(d) and 9(d). The improvement of nitrogen rejection is much more important than the decrease in flux, since the ultimate goal is drinking water production. Thus, naturally occurring hydrolysis of urea is advantageous for production of potable water using RO. It also appears that the ESPA membrane provides the best combination of high rejection and high flux, regardless of the form of the nitrogen compounds in the wastewater.

4. Theoretical model to predict performance

Although the focus of this research was experimental, we applied the classical solution–diffusion (SD)

model modified with the concentration polarization theory to aid in interpreting the experimental results and to predict membrane performance over a wide range of conditions. The solvent flux (J_v) and the solute flux (J_s) through the membrane are [20]:

$$J_v = L_v(\Delta P - \Pi(C_m) + \Pi(C_p)) \quad (3)$$

$$J_s = L_s(C_m - C_p) \quad (4)$$

where L_v and L_s are the solvent and solute transport parameters, C_m and C_p are the solute concentrations at membrane surface and permeate side, $\Pi(C_m)$ and $\Pi(C_p)$ are the osmotic pressures at the solute concentrations of C_m and C_p, respectively, and ΔP the transmembrane pressure.

The difference between C_m and C_b (the bulk concentration of solute) results from the concentration polarization phenomenon. On the basis of the film theory and from Fick's law for diffusion, the concentration profile near the membrane surface is:

$$\frac{C_m - C_p}{C_b - C_p} = e^{J_v/k} \quad (5)$$

where k is the mass transfer coefficient for the back diffusion of the solute from the membrane to the bulk solution on high pressure side of membrane [21]. In a stirred cell, the growth of the concentration boundary layer is limited by stirring according to the mass transfer coefficient [22]:

$$k = 0.104\left(\frac{D_{sw}}{r}\right)\left(\frac{\omega r^2 \rho}{\mu}\right)^{2/3}\left(\frac{\mu}{\rho D_{sw}}\right)^{1/3} \quad (6)$$

where r is the stirring radius, ω the stirring speed, ρ the solution density, and D_{sw} the diffusion coefficient of solute. Rearranging Eq. (5), the solute concentration at the membrane surface can be estimated from the solute concentration of bulk phase.

In stirred cell filtration, J_v, C_b, and C_p are not constant because the volume of concentrate (V_c) changes continuously. The time rate of change of C_b and V_c for a membrane of area A_m are given by

$$\frac{d(C_b V_c)}{dt} = -J_v A_m C_p \quad (7)$$

$$\frac{dV_c}{dt} = -J_v A_m \quad (8)$$

Table 4
Comparison of experimental values of solvent transport parameter with vendor data

Membrane	L_v (Measured)	L_v (Manufacture) m^2-s/kg
BW30	5.21×10^{-12}	3.00×10^{-12}
ATFRO	2.03×10^{-11}	1.37×10^{-11}
ATFRO-HR	1.12×10^{-11}	8.14×10^{-12}
ESPA	1.17×10^{-11}	8.14×10^{-12}
HR95	1.08×10^{-11}	8.33×10^{-12}
NTR729HF	1.42×10^{-11}	5.55×10^{-12}
ACM4	1.81×10^{-11}	9.92×10^{-12}

with the initial conditions $C_b = C_f$ and $V_c = V_f$ at $t = 0$, where C_f and V_f are the initial feed concentration of solute and feed volume, respectively.

Using the average value of permeate concentration defined as $\overline{C_p} = \overline{J_s}/\overline{J_v}$, the average rejection from t_1 to t_2 can be written as using Eq. (2):

$$R = 1 - \frac{[1/(t_2 - t_1)]\int_{t_1}^{t_2} L_s(C_m - C_p)dt}{[C_f/(t_2 - t_1)]\int_{t_1}^{t_2} L_v \Delta P_{eff}\, dt} \quad (9)$$

where ΔP_{eff} is the effective transmembrane pressure $(\Delta P - \Pi(C_m) + \Pi(C_p))$.

Using the above equations, L_v and L_s can be obtained from experimental data to model the rejection under a variety of conditions. L_v is easily determined from the measured pure water flux and Eq. (3). The measured transport property is compared with vendor performance data in Table 4. The measured L_v is somewhat greater than that specified by the manufacturer, but reasonable given that the manufacturers' data are for spiral wound modules which typically have additional pressure losses compared to a stirred cell. It is well known that the properties of the membrane can deviate substantially from the manufacturer's specification [21].

L_s is somewhat more difficult to estimate because the solute concentration at the membrane surface (C_m) is not known. To begin, a line is fit to the experimentally measured solvent flux to obtain an expression for J_v as a function of time, and k is calculated using Eq. (6). Next, Eq. (5) is solved for C_m using the measured value for $J_v(t = 0)$ with initial conditions that the permeate concentration is zero ($C_p = 0$) and the bulk concentration is equal to the initial solute concentration of the feed ($C_b = C_f$). Then an iterative process is used to find the value for L_s with the goal

to match the measured rejection. An initial guess for L_s is used in Eq. (4) to calculate J_s. This is used to calculate $C_p = J_s/J_v$ at the next time step. Then finite difference forms of Eqs. (7) and (8) are used to calculate V_c and C_b at the next time step. C_m is calculated using Eq. (5). The calculations at this time step are completed with the calculation of the integrands of Eq. (9). This process is repeated for the next time step beginning with the calculation of J_s from Eq. (4). The iterative process is repeated for enough time steps to model the full duration of the experiment and provide the value of integrands of Eq. (9) as a function of time. These are integrated according to Eq. (9) to calculate the rejection corresponding to the initial guess for L_s. This process is repeated using a new guess for L_s until the calculated rejection matches the experimentally measured rejection. Once L_v and L_s are found for a set of experimental conditions, they can be used to calculate the rejection at other conditions.

L_v and L_s were calculated for a standard operating condition of $\Delta P = 800$ kPa and $\omega = 400$ rpm for the ESPA membrane, which appears to be the optimal membrane for the wastewaters considered here. The solvent transport parameter is 2.0×10^{-11} m/Pa-s. The solute transport parameters for NaCl and urea for Wastewater A are 1.0×10^{-7} and 2.4×10^{-6} m/s, respectively. The solute transport parameters for NaCl and $(NH_4)_2CO_3$ and for Wastewater B are 1.6×10^{-7} and 8.5×10^{-8} m/s, respectively. Using the empirical values for L_v and L_s, the rejections estimated from the model were compared to the experimental rejections under different operating conditions. The transmembrane pressure ranged from 600 to 1200 kPa, and the stirring speed was varied from 100 to 600 rpm. As demonstrated in Fig. 10, the measured rejection matches the model results quite well for all experimental conditions (points are very near the diagonal line), indicating that the model works well.

The rejections of NaCl and total nitrogen were calculated based on the model as a function of stirring speed and effective transmembrane pressure, which is defined as the difference between transmembrane pressure and osmotic pressure at concentration factor of 2.5. (The effective transmembrane pressure as we defined here can be less than 0. In this case, a concentration factor of 2.5 cannot be achieved). The osmotic pressures at a concentration factor of 2.5 were estimated to be 410 kPa for Wastewater A and 560 kPa for Wastewater B.

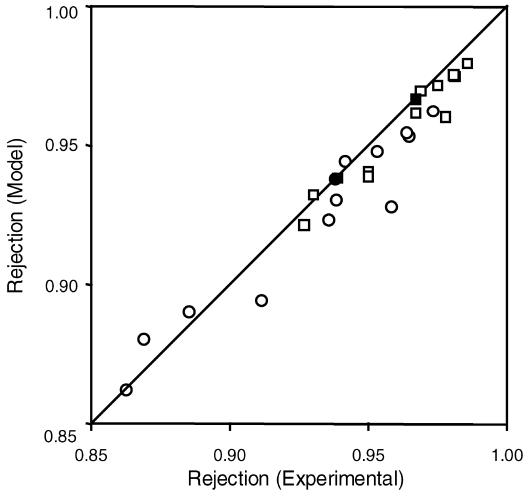

Fig. 10. Comparison of experimental and theoretically estimated rejection for synthetic Wastewaters B (containing NH_4^+). The filled symbol corresponds to the condition at which the modeling parameter (L_s) was determined. ((○): NaCl; (□): TN).

Fig. 11 shows contours of constant rejection of ions and nitrogen for both wastewaters as a function of stirring speed and effective transmembrane pressure. As expected, the best rejection occurs at high stirring speeds and high transmembrane pressures. However, the dependence of rejection on stirring speed and transmembrane pressure is not linear. The closely spaced contours at low stirring speeds and low transmembrane pressures indicate a much stronger dependence under these conditions. This suggests that optimal operating conditions are near the elbow of the contours at moderate stirring speeds and transmembrane pressures rather than at extreme values for these conditions. For instance, the ion rejection for Wastewater B (Fig. 11(c)) is about 0.94 at 300 kPa transmembrane pressure and 300 rpm. Tripling the effective transmembrane pressure increases the rejection by less than 1%. Likewise, tripling the stirring speed only raises rejection to a little over 0.95. Tripling both transmembrane pressure and stirring speed only brings the rejection to a little over 0.97.

The ion rejection is similar for both Wastewaters A and B. However, nitrogen rejection is quite different, reflecting the inherently better rejection of ions

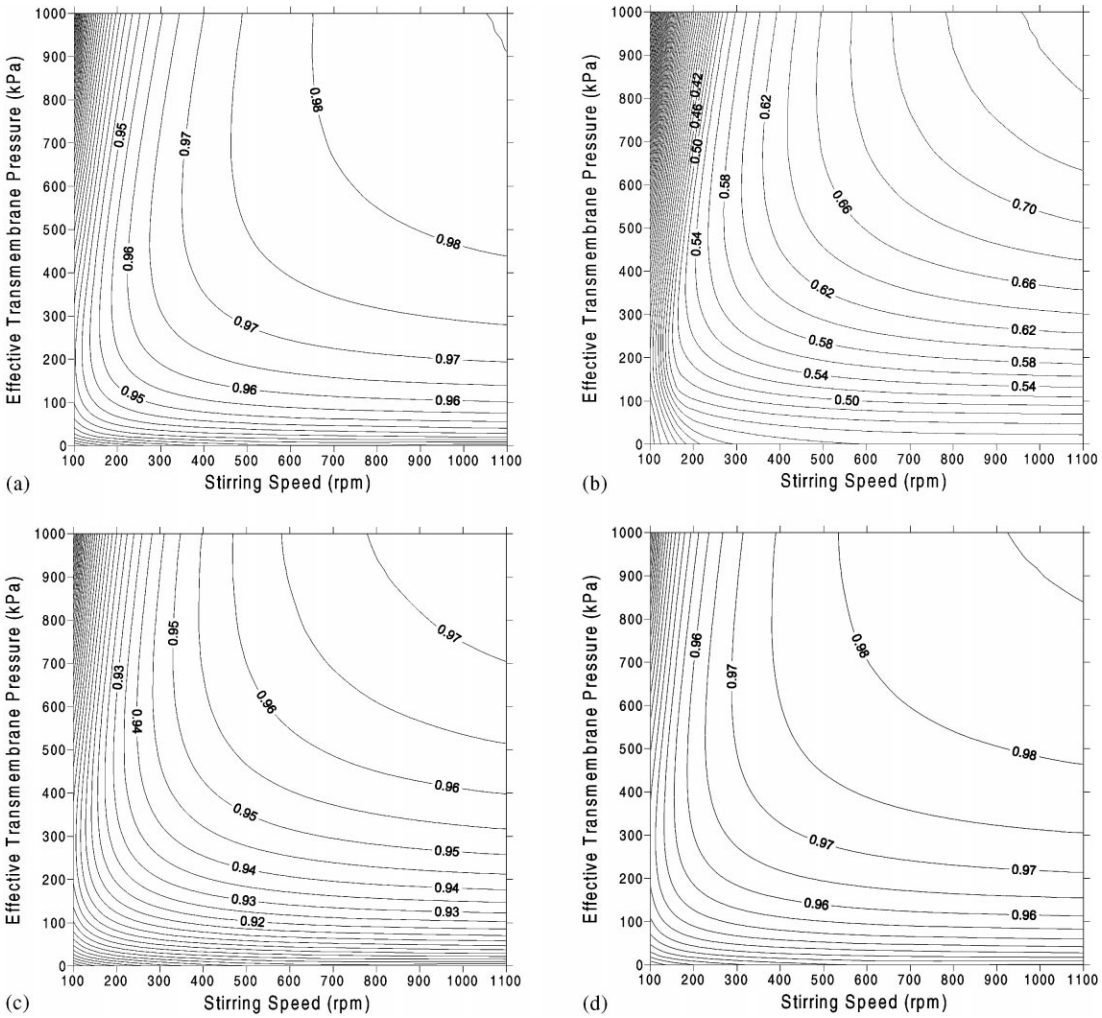

Fig. 11. Contour diagrams of NaCl and total nitrogen rejection at different pressures and stirring speeds. Modeling condition: Membrane, ESPA; concentration factor, 2.5 (a) NaCl rejection for Wastewater A; (b) TN rejection for Wastewater A; (c) NaCl rejection for Wastewater B; (d) TN rejection for Wastewater B.

than organic molecules by the membrane. Regardless of operating condition the rejection of ammonium is well over 0.90 for Wastewater B. The rejection of urea is substantially less. It ranges from below 0.40 at low transmembrane pressures and stirring speeds to 0.74 at high transmembrane pressures and stirring speeds.

An increase in the stirring speed always results in higher rejection for both wastewaters, although the effect is more important in Wastewater A than Wastewater B. For example, an increase of stirring speed from 200 to 400 rpm at effective transmembrane pressure of 400 kPa shows an increase of TN rejection from 0.53 to 0.61 for Wastewater A and that from 0.96 to 0.973 for Wastewater B (Fig. 11(b) and (d)). Of course, the increased rejection occurs because the solute concentration polarization near membrane surface decreases with an increase in stirring speed. The difference between Wastewaters A and B can be attributed to the different values of permeate flux. The flux for

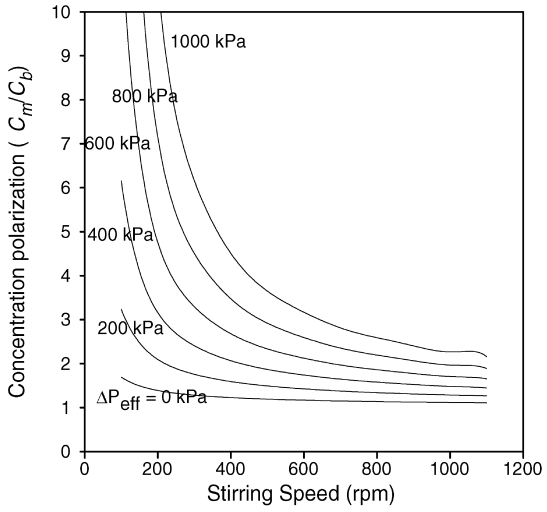

Fig. 12. Effect of stirring speed on concentration polarization. Modeling condition: membrane, ESPA; concentration factor, 2.5; TN for Wastewater B.

Wastewater A is higher than that for Wastewater B, resulting in higher transport of solute to the membrane and greater concentration polarization. Consequently, increased stirring speed is more effective in improving rejection by reducing the concentration polarization for Wastewater A than for Wastewater B.

Increasing the transmembrane pressure at high stirring speeds results in increased rejection for both wastewaters. However, increasing the transmembrane pressure does not improve the rejection at low stirring speed. For example, NaCl rejection at 100 rpm for Wastewater A (Fig. 11(a)) decreases for transmembrane pressures higher than 200 kPa. This can be attributed to the permeate flux being an important factor in addition to concentration polarization. According to solution–diffusion model, the solute rejection should be increased by an increase in solvent flux related to an increased transmembrane pressure. But increased solvent flux also results in greater concentration polarization. The effect of permeate flux without concentration polarization dominates at high stirring speeds. However, the effect of increased concentration polarization with increased permeate flux becomes important at low stirring speeds.

Fig. 12 shows the effect of stirring rate on the concentration polarization ratio (C_m/C_b) at the membrane surface based on the model calculation. The calculation for TN rejection for Wastewater B is presented as an example. The concentration polarization ratios in the figure are averaged values over the course of simulated experiments. If there were no concentration polarization, the concentration polarization ratio would be unity. For high transmembrane pressures the concentration polarization is quite high at low stirring speeds. But the concentration polarization is sharply reduced at stirring speeds above 300 rpm. Even at low transmembrane pressures, stirring reduces the concentration polarization significantly. The practical limit of the stirred batch cell is 600 rpm, so even at the maximum stirring speed, the solute concentration on membrane surface is three times higher than bulk concentration when effective transmembrane pressure is 1000 kPa. The mass transfer coefficient of the stirred cell at 600 rpm is smaller than some commercial membrane modules but has same order of magnitude. Thus, other means of introducing a high shear could be used in order to further reduce concentration polarization to obtain higher rejection. Dynamic rotating membrane filtration, which can produce a high shear rate [23], may be helpful to obtain high rejection of organic pollutants. The rotation of the filter gives rise to a high shear (equivalent to a high stirring speed), which could significantly lower the concentration polarization in RO filtration.

5. Conclusion

In this work, a preliminary study of the application of RO membranes to a wastewater reuse system for spacecraft use was performed using laboratory scale experiments. The following conclusions can be drawn:

1. Several RO membranes were compared in terms of permeate flux and solute rejection. LPRO membranes are most effective to recover wastewater with high flux and high solute rejection, regardless of whether they are Category I or II membranes.
2. Even though very high rejection of detergent and dissolved ions was obtained by RO, the rejection of TOC and urea was lower. This is because the chemical affinity between solutes and the membrane is much more important than the size exclusion effect.

3. Urea hydrolysis, which is a common process during storage, plays a significant role in nitrogen rejection. The nitrogen rejection increased significantly after urea hydrolysis, since ammonium ions are more easily rejected by RO membranes than urea.
4. Hydrodynamic operating conditions greatly affect the rejection of solutes in RO treatment. The rejection of organic nitrogen compounds should increase with increased shear rates near membrane surface. This suggests that the rejection will be further improved using dynamic membrane filtration.

Acknowledgements

This work was supported by NASA (NASA grant NAG9-1053). The authors thank Ms. Karen Pickering for her support and advice regarding the filtration experiments. The authors also thank Dr. Deanna Hurum and Ms. Tanita Sirivedhin for their help in chemical analysis at the Civil and Environmental Engineering Department, Northwestern University. The authors also thank Hydranautics Inc. and Advanced Membrane Technology, Inc. for their donation of membrane samples.

References

[1] NASA Lyndon B. Johnson Space Center, Advanced life support program requirements definition and design considerations, CTSD-ADV-245 (Rev A), Houston, TX 77058, 1998.
[2] P. Weiland, Design for human presence in space, NASA RP-1324, 1995.
[3] T.J. Salavin, M.W. Oleson, Technology tradeoffs related to advanced mission wastewater processing, Waste Manage. Res. 9 (1991) 401–414.
[4] R.C. Cooper, The hygiene aspects of wastewater reuse, Waste Manage. Res. 9 (1991) 373–377.
[5] R.B. Dean, Processes for water reclaimation, Waste Manage. Res. 9 (1991) 425–430.
[6] B.W. Finger, L.N. Supra, L. DallBauman, K.D. Pickering, Development and testing of membrane biological wastewater processors, in: Proceedings of International Conference on Environmental Systems, SAE paper 1999-01-1947, 1999.
[7] A.D. Williams, C.S. Slater, Recovery of wastewater in microgravity (space) applications using pervaporation processes and volatile rejection membranes, in: Proceedings of the Fifth International Conference on Pervaporation Processes, Bakish Materials Publishers, Englewood, NJ, 1991, pp. 383–391.
[8] D. Parker, ISS water reclamation system design, in: Proceedings of International Conference on Environmental Systems, July 1999, Denver, CO, USA, Session: International Space Station ECLSS I System Aspects & Water, 1999-01-1950.
[9] C.S. Slater, C.A. Brooks, III Development of a simulation model predicting performance of reverse osmosis batch systems, Separation Sci. Technol. 27 (11) (1992) 1361–1388.
[10] D.J. Demboski, J.H. Benson, G.E. Rossi, N.S. Leavitt, M.A. Mull, Evolutions in U S navy shipboard sewage and graywater programs, in: Proceedings of the ASNE Environmental Symposium Environmental Stewardship: Ships and Shorelines, November 1997.
[11] S. Lee, C.H. Lee, Effect of operating conditions on scale formation in nanofiltration for water treatment, Water Res. 34 (15) (2000) 156–168.
[12] K.D. Pickering, NASA Johnson Space Center, Houston, TX, Personal communication, 1999.
[13] APHA, AWWA and WEF, Standard Methods for the Examination of Water and Wastewater, 18th Edition, American Public Health Association, Washington, DC, 1992.
[14] Hach Company, Hach Water Analysis Handbook, 2nd Edition, Hach Company, CO, USA, 1992.
[15] J.M.M. Peeters, J.P. Boom, M.H.V. Mulder, H. Strathmann, Retention measurements of nanofiltration membranes with electrolyte solutions, J. Membr. Sci. 145 (1998) 199–209.
[16] J. Schaep, C. Vandecasteele, A.W. Mohammad, W.R. Bowen, Analysis of the salt retention of nanofiltration membranes using the donnan-steric partitioning pore model, Separation Sci. Technol. 34 (15) (1999) 3009–3030.
[17] A.C. Archer, A.M. Mendes, R.A.R. Boaventura, Separation of an anionic surfactant by nanofiltration, Envrion. Sci. Technol. 33 (1999) 2758–2764.
[18] M. Hirose, H. Ito, M. Maeda, K. Tanaka, Highly permeable composite reverse osmosis membrane, method of producing the same, and method of using the same, United States Patent 5, 614, 099, 1997.
[19] V.H. Varel, Use of urease inhibitors to control nitrogen loss from livestock waste, Biores. Technol. 62 (1997) 11–17.
[20] J.G. Wijmans, R.W. Baker, The solution–diffusion model: a review, J. Membr. Sci. 107 (1995) 1–21.
[21] M. Cherayan, Ultrafiltration and Microfiltration Handbook, Technomic Publishing Co., Lancaster, Basel, 1998.
[22] S. Nicolas, B. Balannec, F. Beline, B. Bariou, Ultrafiltration and reverse osmosis of small non-charged molecules: a comparison study of rejection in a stirred and an unstirred batch cell, J. Membr. Sci. 164 (2000) 141–155.
[23] R.M. Lueptow, A. Hajiloo, Flow in a rotating membrane plasma separator, Am. Soc. Artif. Int. Organs J. 41 (1995) 182–188.